Published for SISSA by Springer

Received: *September 11, 2023*
Revised: *October 18, 2023*
Accepted: *October 23, 2023*
Published: *November 20, 2023*

Third order QCD predictions for fiducial W-boson production

John Campbell[a] **and Tobias Neumann**[b]

[a] *Fermilab,*
PO Box 500, Batavia, Illinois 60510, U.S.A.
[b] *Department of Physics, Brookhaven National Laboratory,*
Upton, New York 11973, U.S.A.

E-mail: johnmc@fnal.gov, tneumann@wm.edu

Abstract: Measurements of W-boson production at the LHC have reached percent-level precision and impose challenging demands on theoretical predictions. Such predictions directly limit the precision of measurements of fundamental quantities such as the W-boson mass and the weak mixing angle. A dominant source of uncertainty in predictions is from higher-order QCD effects. We present a calculation of W-boson production at the level of α_s^3 at fixed order and including transverse-momentum resummation. We further show predictions for a direct comparison with low-pileup ATLAS transverse-momentum and fiducial cross-section measurements at $\sqrt{s} = 5.02\,\text{TeV}$. We discuss in detail the impact of modern PDFs. Our calculation including the matching to W+jet production at NNLO will be publicly available the upcoming CuTe-MCFM release and allows for theory-data comparison at the state-of-the-art level.

Keywords: Higher-Order Perturbative Calculations, Parton Distributions

ArXiv ePrint: 2308.15382

https://doi.org/10.1007/JHEP11(2023)127

Contents

1 Introduction

The production of W bosons at hadron colliders has one of the highest cross-sections of all Standard Model (SM) processes. Together with its relative ease of detection, through a large branching ratio into a lepton and neutrino, it has been measured with very high precision at multiple colliders. At the LHC, measurements range from center of mass energies of 2.76 TeV to 13 TeV, as performed by ATLAS [1–4], CMS [5–9] and LHCb in the forward region [10–14]. Since the first measurements at the LHC, luminosity uncertainties have reduced from 2–3% to 1% [15, 16], setting the upper bound on the precision reached in current measurements [17].

The precision of these analyses opens the door to the measurement of fundamental quantities appearing in the weak sector of the SM Lagrangian, such as the W-boson mass [18–23], the weak mixing angle, as well as stringent constraints on parton distribution functions (PDFs) [4, 24, 25] and charge asymmetries [9, 26–29].

However, the interpretation of these measurements — and their ultimate precision — depends crucially on the sophistication of the theoretical predictions with which they are compared and analyzed. First N^{3}LO predictions for W-boson production have been presented for total inclusive cross-sections in ref. [30] (and in ref. [31] for Z), where large cancellation effects between initial-state channels have been observed that lead to significant N^{3}LO corrections of about -2.5%.

Fixed-order α_s^3 W+jet predictions [32] (NNLOjet) have been matched to the RadISH resummation [33, 34] in ref. [35] at the level of N^{3}LL and compared to Pythia results. Similar results have been achieved for Z production [35–39]. Higher-order transverse-momentum resummation at the level of N^{3}LL' matched to lower-order α_s^2 predictions has also been

JHEP11(2023)127

studied in refs. [40, 41]. Recent studies of threshold resummation in rapidity distributions were presented in refs. [42–45]. Transverse-momentum resummation is also considered with a focus on TMD fits in the literature [46]. Fixed-order N^{3}LO predictions for W-boson production have been presented in ref. [47] (transverse mass distribution, rapidity, charge asymmetry), which also includes a Tevatron study using fiducial cuts.

Generally the residual QCD truncation uncertainties at the level of α_s^3 are estimated to be at the level of $1-2\%$. Apart from QCD effects, other Standard Model effects play a role at the level of 1% precision. Among these, mixed QCDxEW corrections were reported in refs. [48–52] and QED- QCD transverse-momentum resummation in ref. [53].

While all of these recent higher-order corrections are important for percent-level comparison with kinematic measurements, they are crucial to improve the W-boson mass measurement. In particular, even though few measurements have been performed of the W-boson transverse momentum directly [17, 54, 55], it is a key part in the W-boson mass analyses. A comprehensive review of how theoretical contributions and uncertainties impact the W-boson mass measurement was presented in ref. [56] (2016), while the impact of PDF [57] and higher-order [58] uncertainties have also been separately assessed more recently. An estimate for the impact of mixed QCDxEW corrections has since also been performed [59].

In this paper we present a calculation of fully differential W-boson production at N^{3}LO fixed-order and including transverse-momentum resummation up to a logarithmic order of N^{4}LL matched to N^{3}LO fixed-order.[1] Together with our calculation of Z production at α_s^3 [39], it completes the set of two crucial processes entering many Standard Model precision analyses in CuTe-MCFM, for example the W-boson mass determination. It allows for QCD predictions at the highest level with an independent implementation of higher-order ingredients and resummation. The availability of multiple calculations in different resummation formalisms enables reliable uncertainty estimates. In this paper we compute predictions for comparison with the $\sqrt{s} = 5.02\,\text{TeV}$ ATLAS analysis from ref. [17]. The calculation will be made publicly available, so that its results can be used for future analyses, in the upcoming release of CuTe-MCFM.

In section 2 we describe our setup and cross-checks performed on our calculation. In section 3.1 we first discuss predictions of the fiducial cross-section and compare with the measurement. In particular we focus on the impact of PDFs. We move on to differential distribution in section 3, where we discuss the W-boson transverse-momentum distribution (section 3.2) and transverse mass and charged lepton transverse-momentum distributions (section 3.3). Since the impact of PDFs is significant, we discuss their impact on these distributions in section 3.4. We conclude and present an outlook in section 4.

2 Setup

We implement QCD corrections to $pp \to W(\to e\nu)$ production at fixed-order and including the effect of q_T-resummation in CuTe-MCFM [39, 60–62]. We achieve α_s^3 fixed-order and

[1] The logarithmic accuracy of N^{4}LL is only reached within the limitations of current N^{3}LO PDF approximations and without the contribution from the five-loop cusp anomalous dimension.

JHEP11(2023)127

transverse momentum renormalization-group-improved (RG-improved) logarithmic accuracy, counting $\log(q_T^2/Q^2) \sim 1/\alpha_s$. Note that the logarithmic accuracy of N^{4}LL (α_s^3) relies on the availability of N^{3}LO PDFs, in particular on the four-loop DGLAP evolution. PDFs at this order are so far only available by the MSHT group in an approximation [63]. The ingredients of our calculation and the checks we have performed are detailed below.

Resummation. The implementation of the resummation formalism follows our study on Z production [39], it is based on the SCET-derived q_T-factorization theorem developed in refs. [64–66] and originally implemented to N^{3}LL as CuTe-MCFM in ref. [60]. Large logarithms $\log(q_T^2/Q^2)$ are resummed through RG evolution of hard- and beam functions in a small-q_T factorization theorem. Rapidity logarithms are directly exponentiated through the collinear-anomaly formalism.

The transition from the resummation which is valid only at small q_T, to fixed-order predictions at large q_T, is achieved through the use of a transition function that smoothly interpolates between those two regions [60]. The overlap between fixed-order and resummation is removed through a fixed-order expansion of the factorization formula. The difference between these two parts is referred to as matching corrections. While for Z production matching corrections quickly approach zero for $q_T \to 0$, even at the level of α_s^3, we find that for W production they are at the level of a few percent even at relatively small q_T (as described in detail in section 2.1 below).

The higher-order ingredients in the resummation calculation are identical to those in Z production. We briefly summarize the most important ones here, and refer for more details to our implementation of Z production [39]. Three loop transverse momentum dependent beam functions that allow for resummation at the level of N^{3}LL' have been calculated in refs. [67–69]. We include the four loop rapidity anomalous dimension [70, 71], which together with N^{3}LO PDFs allows for N^{4}LL resummation. The five-loop cusp anomalous dimension needed at N^{4}LL is numerically negligible, which is true already at the four-loop level.

The formalism of refs. [64–66] further employs an additional power counting that improves the resummation at small q_T [65] and avoids a Landau pole prescription, as the relevant scales are always set in the perturbative regime. Implementing this requires the inclusion of higher-order terms of the beam functions which were reconstructed from the beam-function RGEs in ref. [39].

The hard function entering the factorization formula consists of $\overline{\text{MS}}$-renormalized virtual corrections. For Z production these are more complicated due to separate singlet and axial-singlet contributions, which are not present for W production. The hard function is therefore solely given by the three-loop (vector) form-factor [72–74].

Fixed order. To obtain fixed-order N^{3}LO results we use q_T slicing [75], which was implemented in ref. [39] using the same factorization theorem and ingredients as laid out above for the resummation.

The W+jet NNLO calculation, which is necessary above the q_T slicing cutoff, is based on ref. [76] using 1-jettiness subtractions [76–78] and the 1-jettiness soft-function of refs. [79, 80]. We have thoroughly cross-checked all elements of this calculation. For example,

JHEP11(2023)127

we find agreement between all amplitude expressions and Recola [81]. Further checks were performed as part of the validation of Z+jet production, for example a re-implementation of the non-singlet hard function using refs. [82–84] that was originally taken from the code PeTeR [85, 86]. We have identified and corrected small inconsistencies in the original implementation of NLO subtraction terms in the $W + 2$ jet process [87], a component in our above-cut calculation. We have further checked our final NNLO W+jet results against a fully independent calculation presented in ref. [88].

2.1 Cutoff effects and uncertainties

We study fixed-order and resummed results, which are both affected by cutoff effects in different ways. The resummed calculation requires a cutoff of the matching corrections, while our N^{3}LO fixed-order calculation is based on a nested slicing approach, regularizing N^{3}LO singularities using q_T subtractions. In both cases the NNLO W+jet calculation is performed using 1-jettiness slicing, and therefore, unlike for the local antenna subtractions used in the NNLOjet calculation [32], we have to particularly pay attention to residual slicing cutoff effects.

For the plots here and throughout the results section, we use the cuts of a recent ATLAS study [17] shown in eq. (3.1) in section 3. The choice of symmetric q_T cuts on the W decay leptons makes the calculation numerically challenging [38, 47], even when including linear power corrections in the q_T slicing method.

Unlike for Z-boson production [39] the cutoff effects are not negligible at the order of α_s^3 for cutoff values of 3 GeV to 5 GeV that we achieve here. We therefore take care to display the limitations of this throughout our results.

Cutoff effects in the resummation. We first discuss cutoff effects in the matched resummed result. In figure 1 we show the matching corrections relative to the purely resummed α_s^3 result at different orders in α_s. While they are small and quickly approach negligible levels at lower orders, the α_s^3 corrections are substantial.

At lower orders we use a matching corrections cutoff of 1 GeV, with negligible impact on the results, while at α_s^3 we use a cutoff of 3.16 GeV and a q_T-dependent dynamic jettiness cutoff of the NNLO W+jet calculation of $\frac{0.03}{1050}\sqrt{q_T^2 + m_{ll}^2}$, so about 0.002 GeV at small q_T. Lower values of q_T would require smaller values of a jettiness cutoff, significantly increasing computational resources.

From figure 1, the matching corrections are still above 3% around our cutoff of 3.16 GeV. We estimate the uncertainty due to missing matching corrections by multiplying the purely resummed result integrated up to 3.16 GeV by three percent. The impact of this is different in various kinematical distributions and also depends on the binning. For example in the W-boson q_T distribution in ATLAS binning [17] the first bin ranges from 0 GeV to 7 GeV. The effect of neglected matching corrections in this bin is up to about 1.5%, while there is no such error in the other bins. Overall, the effect of neglecting matching corrections is therefore not negligible and needs to be included in uncertainty estimates.

JHEP11(2023)127

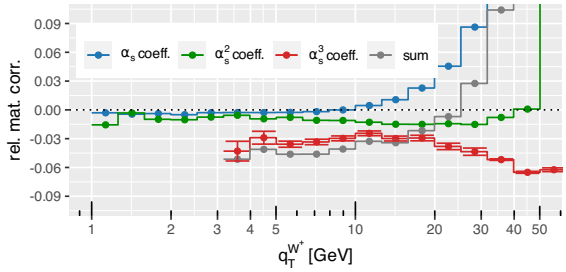

Figure 1. Matching corrections for W^+ production at $\sqrt{s} = 5.02\,\text{TeV}$ with fiducial cuts as in section 3. The error bars at α_s^3 denote the estimated integration uncertainty.

In distributions other than the W-boson q_T this effect is smeared out and we include it as an additional error bar. Since we know that the effect is likely to lead to a reduction of the cross-section, we display the error bar only in the downwards direction.

Perturbative truncation uncertainties. Uncertainties associated with missing higher order effects are estimated by performing scale variations following the procedure of ref. [39] for the Drell-Yan process. This includes a variation of a number of scales. We vary a (low) resummation scale by a factor of two around its nomial value of $\sim q_T$ (see ref. [60] for details), a hard scale in the resummation ($\sim m_W$) by a factor of two, and the rapidity scale in the resummation by a factor of six (tuned on the truncation of the improved power counting in the resummation formalism, see ref. [62]). The usual variation of renormalization and factorization scale in the fixed-order part is by a factor of two around $\sqrt{m_{l\nu}+q_{T,l\nu}^2}$ and is dominated by the simultaneous excursion of both scales.

Our matched resummed results also account for uncertainties in the transition function, which is needed to switch between the resummed and fixed-order calculations and is determined by the size of the matching corrections (figure 1). The matching corrections become sizeable beyond 40 GeV, which motivates a transition function as detailed in ref. [60] using $x_T^{max} = (q_T^{max}/M_Z)^2$ with q_T^{max} in the range 35 to 60 GeV. With this choice we find that transition uncertainties, obtained by varying the transition function ($x_T^{\text{max}} = 0.2, 0.4, 0.6$), are then comparable to uncertainties in the fixed-order and resummation regions. They are therefore insensitive to the precise range and shape of the transition.

We combine uncertainties by taking the maximum excursion of the individual uncertainties and symmetrize them. These uncertainties are computed for both differential and total fiducial results. In the differential plots they are represented by the colored shaded bands.

Cutoff effects at fixed order. Our NNLO and N^{3}LO fiducial fixed-order cross-sections are computed using q_T slicing. For the resummed calculation linear power corrections are included automatically through a recoil prescription [89–91]. In the fixed-order case they have to be added separately, although this is straightforward [92].

The size of the linear power corrections for the α_s^k coefficient relative to the full α_s result is shown in figure 2 for W^+production, as a function of the q_T slicing cutoff, q_T^{cut}.[2] At

[2]The relative power corrections for W^- production are virtually identical.

JHEP11(2023)127

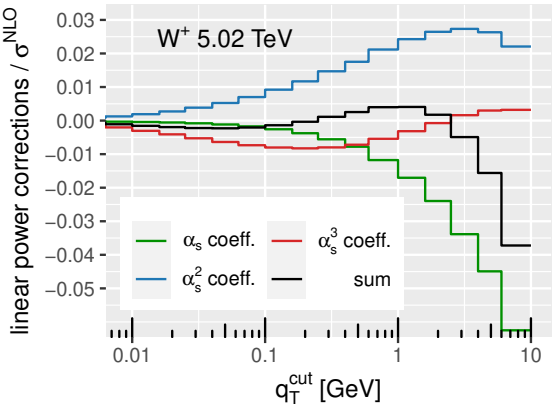

Figure 2. Linear power corrections for $W^{\pm}$ production at $\sqrt{s} = 5.02\,\text{TeV}$ relative to the NLO cross-section, with input parameters as in section 3.

NNLO we use a q_T slicing cutoff of 1 GeV with linear power corrections on the cross-section at the level of 2%. For the N^{3}LO coefficient we use a cutoff of 3.16 GeV and the power corrections are a few per-mille. The large size of the power corrections is an effect of the symmetric lepton cuts [38].

To demonstrate that cutoff effects are well under control at NNLO we display the q_T^{cut} extrapolation for the fiducial NNLO coefficient in figure 3 (left) with and without included linear power corrections (figure 2). The inclusion of power corrections allows for a 1 GeV cutoff with negligible uncertainty. The cutoff is deep in the asymptotic region so that even in differential distributions this cutoff is justified. It is also clear that the linear power corrections are crucial in order to reach this conclusion. Without them the asymptotic result has not even been reached at 1 GeV and a stable fit is not possible. This again traces back to the choice of symmetric lepton cuts.

Our final fiducial N^{3}LO corrections are obtained from a q_T^{cut} extrapolation, taking into account that subsequently smaller τ_{cut} values are necessary for small q_T^{cut} in the inner W+jet NNLO calculation. This is shown in figure 3 (right) for W^+ production. The overall pattern is that for too large τ_{cut} the cross-section diverges towards more negative values.

The dependence for W^- is qualitatively the same. Note that the τ_{cut} dependence is modified by the dynamic choice, our default is $\tau \propto \sqrt{q_T^2 + m_{ll}^2}$. Other choices for the functional dependence of τ, such as $\tau \propto q_T$, may lead to improved performance. We leave a detailed investigation of such choices to a future publication.

The solid red line is from one possible fit of the expected asymptotic behavior. We estimate the uncertainty of the asymptotic fit by varying the number of terms that are included in it. The leading asymptotic behavior includes terms of the form $q_T \cdot \log(q_T^2)^n$ with $n = 5$ and lower, as well as a constant asymptotic term. We further check the insensitivity to the data that are included and find that the fit result is stable under removing the first three data points, where then the fit starts at a cutoff of 6 GeV. Therefore, we are not affected by the first point which might not be fully asymptotic in τ_{cut}. Overall, we find a fit uncertainty of about 4–5 pb. In addition to the fit uncertainty, the red error bar denotes our numerical uncertainty of about 4 pb that affects all points.

JHEP11(2023)127

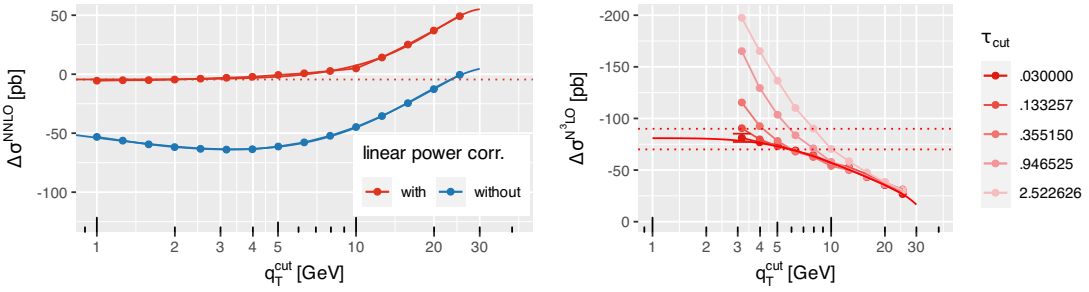

Figure 3. Left: q_T^{cut} extrapolation of the fiducial NNLO W^+ cross-section coefficient at 5.02 TeV with and without linear power corrections. The dotted red line shows the asymptotic fit value when including these power corrections. Right: q_T^{cut} and τ_{cut} extrapolation of the fiducial N^{3}LO W^+ cross-section coefficient at 5.02 TeV (not including the small linear power corrections). The error bar denotes the estimated numerical uncertainty. The solid red line is the result of a fit. The dotted red lines are an estimate of our overall uncertainty.

In total we assign a 10 pb technical uncertainty on the fiducial cross-section, which is visualized by the dotted red bars in figure 3 (right). Our central value of the N^{3}LO coefficient is -80 ± 10 pb. This uncertainty in the N^{3}LO coefficient translates into a 0.5% uncertainty in the full cross-section.

As an additional check of our setup we worked to reproduce the total inclusive cross-section that can be calculated conveniently with the code `n3loxs` [30, 93]. At NNLO using a 1 GeV cutoff our agreement is better than 0.1%, and achieving this precision was even challenging with `n3loxs` which underestimated uncertainties in some runs. At N^{3}LO we find agreement, but unfortunately this calculation is numerically particularly challenging in our nested slicing approach. In the fiducial case the power corrections are more manageable, which allowed us to obtain results with a numerical and slicing error of less than 0.5%. In the total inclusive case the power corrections are larger, but also the numerical integration turns out to be more difficult. We find agreement within a combined uncertainty of about 1%. Given that the total N^{3}LO corrections are about -1.7% for the choice of invariant mass range and input parameters that we took, this is not as strong of a cross-check as we would have liked.[3] We also computed the total inclusive cross-section including the effect of q_T resummation and find an inconclusive difference of $-1.8\% \pm 1.2\%$ (here also an uncertainty from the transition function enters).

We used about 50000 NERSC Perlmutter core hours (64 nodes for 12 hours) to compute the total inclusive N^{3}LO cross-section to the precision of 1%. While these are not huge resources in the context of current calculations [94] which can go into the millions of core hours, reducing the numerical error by a factor of one third would already ten-fold these resource requirements, since Monte-Carlo integration uncertainties decrease like the square root asymptotically. The large power corrections further demand smaller cutoffs to reduce the slicing uncertainty, which also contributes sizeably in the total. Accounting for power corrections in the W + jet NNLO calculation provides a possible path for reducing the overall slicing uncertainty [95, 96]. However, ultimately a more efficient approach such as

[3]The N^{3}LO cross-section obtained with `n3loxs` is 4140 ± 1 pb with ΔN^{3}LO $= -72$ pb, while we find ΔN^{3}LO $= -83 \pm 40$ pb (slicing + numerical error).

JHEP11(2023)127

a local subtraction procedure, and ideally local N^{3}LO subtractions, will be necessary to substantially reduce these uncertainties.

3 Results

In this section we show fiducial cross-sections and distributions for W^+ production at $\sqrt{s} = 5.02\,\text{TeV}$ corresponding to the ATLAS analysis in ref. [17]. The fiducial cuts for this analysis are,

$$\begin{aligned} &q_T^\ell > 25\,\text{GeV}\,, \qquad q_T^\nu > 25\,\text{GeV}\,, \qquad \left|\eta^\ell\right| < 2.5\,, \\ &m_T = \sqrt{2q_T^\ell q_T^\nu(1-\cos\Delta\phi_{\ell\nu})} > 50\,\text{GeV}\,. \end{aligned} \tag{3.1}$$

Note that the theory predictions used in that analysis are at a lower order and do not include any uncertainties. We include the corresponding plots for W^- production in appendix A since overall the relative perturbative corrections are very similar.

For all our predictions we use the G_μ scheme with $m_W = 80.385\,\text{GeV}$, $m_Z = 91.1876\,\text{GeV}$ and $G_F = 1.6639 \times 10^5\,\text{GeV}^{-2}$, as well as $\Gamma_W = 2.091\,\text{GeV}$. Different scheme choices can be used to estimate the effect of higher-order electroweak corrections [97] which we do not consider here. We examine the impact of various PDF sets, extracted at different perturbative orders, in our study and will make clear which PDF set is used in each prediction.

In the following, the label α_s^k at fixed-order denotes N^{k}LO, while for the resummed cross-section it denotes N^{k+1}LL+N^{k}LO, that is α_s^k in an RG-improved power counting where large logarithms $\log(q_T^2/Q^2)$ are counted as $1/\alpha_s$. Note that only the prediction using the `MSHT20an3lo` PDF set [63] reaches approximately N^{4}LL logarithmic accuracy, within the limitations of its approximations. For the NNLO PDF sets the effect from missing four-loop splitting functions degrades the formal accuracy to N^{3}LL', see ref. [39].

As well as the fiducial cross section, we choose to discuss the W-boson transverse momentum, charged-lepton transverse momentum and W-boson transverse mass distributions, which are of particular interest for the W-boson mass analyses.

3.1 Fiducial cross-sections

We start with a discussion of the total fiducial cross-section that we compare with the recent 5.02 TeV ATLAS measurement [17]. We compare predictions of different perturbative orders in α_s at fixed order as well as including the effect of q_T resummation at the respective logarithmic order. Even at the level of the fiducial cross section this is interesting because, in the presence of symmetric lepton q_T cuts such as those in this analysis (cf. equation (3.1)), one expects some difference between resummed and fixed-order predictions due to a strong sensitivity to unphysically low momentum scales [98].

For our theory predictions we match the PDF order with the perturbative cross-section order for consistency, using `MSHT20` PDF fits with $\alpha_s(m_Z) = 0.118$ [63, 99]. This is particularly important for the logarithmic accuracy in the resummation. Uncertainties associated with missing higher order effects are estimated by performing scale variations

JHEP11(2023)127

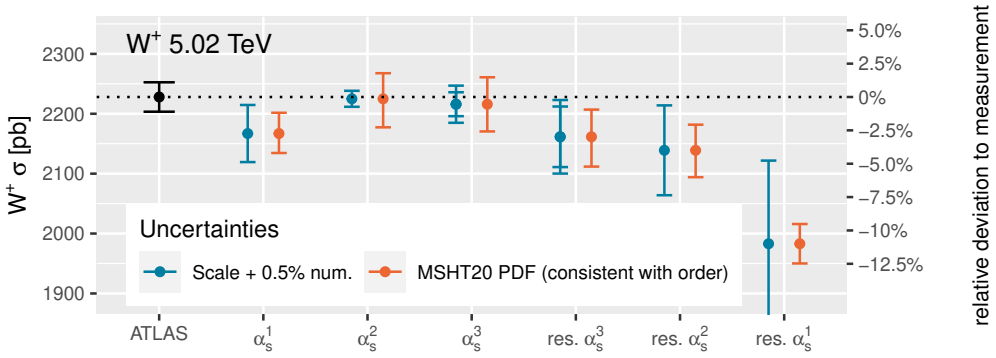

Figure 4. W^+ cross-sections in comparison with the ATLAS 5.02 TeV measurement [17]. Error bars show uncertainties from scale variation and from the MSHT20 PDF sets corresponding to the perturbative order. The α_s^3 results have an additional numerical and cutoff uncertainty of 0.5% that we added linearly to the scale uncertainties for display.

following the procedure of ref. [39] for the Drell-Yan process. These are symmetrized based on the maximum excursion for simplicity. We also take into account uncertainties from the PDF determination, which for the case of the MSHT20 approximate N^{3}LO PDF set [63] accounts for missing higher-order effects within the PDF in addition to uncertainty arising from the fitting procedure. Furthermore, as discussed in section 2.1, our α_s^3 results have an additional uncertainty of 0.5% that covers our remaining uncertainty due to cutoff effects in the slicing procedure and matching corrections.

Our results, and comparison to the ATLAS measurement, are shown in figure 4.[4] We find that perturbative corrections are small for both the fixed-order and resummed results. Ultimately this is due to the effect of the (approximate) N^{3}LO PDFs, which we discuss in the following. Scale uncertainties at N^{3}LO (<1%) are at the level of NNLO uncertainties, which is a feature already observed in the literature in both inclusive and differential cases [30, 47]. On the other hand, scale uncertainties for our resummed results consistently decrease, but are still about 2% at order α_s^3.

The α_s^3 fixed-order and resummed cross-sections are marginally compatible, and overall uncertainties from both predictions are still too large to indicate a significant difference that would indicate the need for resummation [98]. In addition, the experimental precision is limited by about a 1% luminosity uncertainty and is compatibly with both predictions. Of course a direct window on this issue comes from a comparison of predictions with the measurement of the q_T^W distribution since the bulk of the cross-section comes from the region of small q_T where resummation is required. We defer this discussion to section 3.2.

PDF dependence. We now extend our discussion by considering PDFs from different groups, where it is not possible to consistently match the order in α_s of the PDF fit to that of the perturbative calculation. In this section we therefore use the same PDF set at each order of the perturbative calculation. We will compare results using the MSHT20nnlo_as118

[4]We have added the ATLAS systematic and statistical experimental uncertainties in quadrature.

JHEP11(2023)127

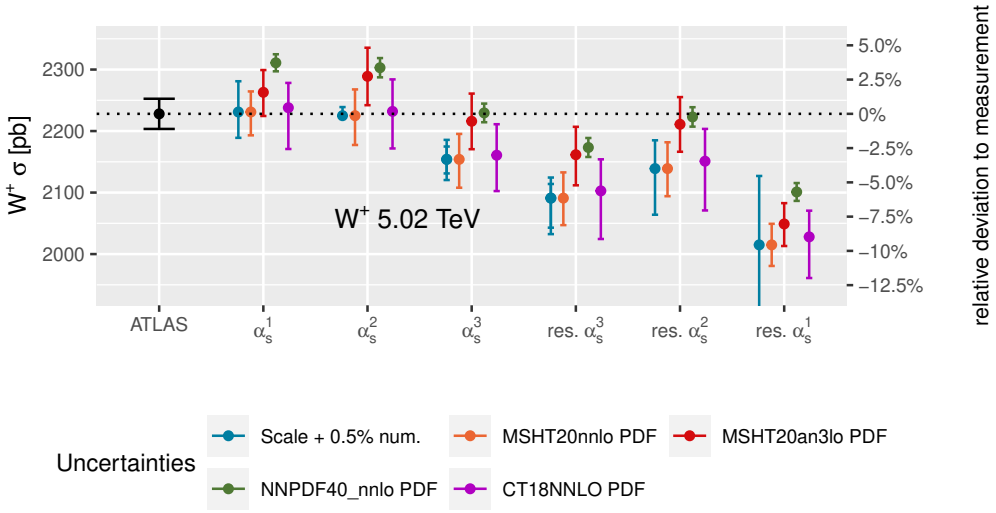

Figure 5. W^+ cross-sections in comparison with the ATLAS 5.02 TeV measurement [17]. Error bars show uncertainties from scale variation and from different PDF sets with their respective uncertainties. The α_s^3 results have an additional numerical and cutoff uncertainty of 0.5% that we have added linearly to the scale uncertainties for display.

PDF set with those from the NNLO determinations `MSHT20nnlo_as118`, `CT18NNLO` [100] and `NNPDF40nnlo_as_0118` [101].

Our results are shown in figure 5. We first focus on the fixed-order and resummed α_s^3 predictions using `MSHT20` at NNLO and aN^{3}LO. Since the same data was used in both PDF fits, the difference between these predictions therefore solely results from higher-order corrections in the PDF and the inclusion of N^{3}LO K-factors in the predictions of some cross-sections. The aN^{3}LO PDF increases the α_s^3 results by about 3% compared to using the NNLO PDF. This is a significant deviation also in terms of the PDF uncertainties. Without taking into account the aN^{3}LO PDFs we would conclude a cross-section decrease of about 3.2% at fixed-order and about 2.3% using the resummed result.[5] This is similar in size to the effects observed in previous calculations of this process more inclusively, where the same PDF set has been employed across all orders of the calculation [30, 47].

The size of the aN^{3}LO PDF effects, and the delicate cancellation between different partonic channels, indicates that a consistent order is important, see also figure 4. On the other hand the `NNPDF4.0` NNLO PDF set is consistent with the larger cross-sections of the `MSHT20` aN^{3}LO PDF. This leads to the question of what impact N^{3}LO effects will have in a `NNPDF4.0` fit. Judging by the pattern in `MSHT20` one would expect a sizeable positive shift, which would lead the fixed-order prediction to overshoot the measurement. From this it is clear that the improvement of PDFs is a priority for precision predictions and measurements of this process.

To conclude the discussion of the fiducial cross-section, we find that theory uncertainties are overall at the level of 3-5% for the α_s^3 W-boson cross-section. This includes scale (truncation) uncertainties, the envelope of PDF uncertainties and the difference between

[5] Note that our numerical and cutoff uncertainty is about 0.5%.

JHEP11(2023)127

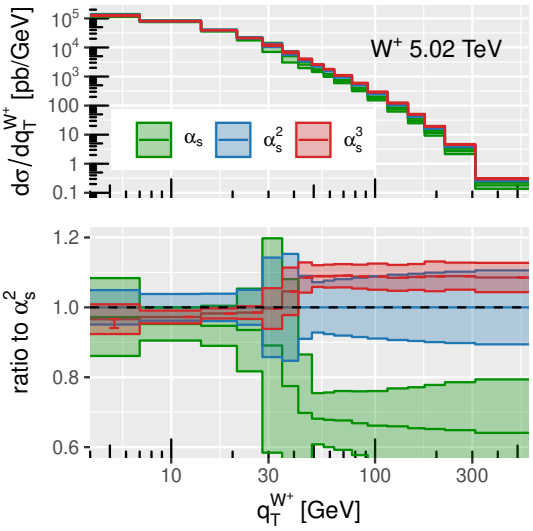

Figure 6. W^+ transverse momentum distribution at 5.02 TeV using the PDF set `MSHT20nnlo_as118` throughout.

fixed-order and resummed results. All individual uncertainties are at the percent level and it will require effort in all directions to significantly reduce the overall theoretical uncertainty. In particular it will require careful investigation of PDFs in terms of higher-order effects and systematics as well as the estimation of statistical uncertainties, which vary significantly between modern PDF sets. The comparison of differential cross-sections is likely to shed further light on these issues, which we discuss further when comparing differential PDF uncertainties in section 3.4.

3.2 Transverse momentum distributions

Moving towards differential quantities, we show the W^+ transverse momentum distribution at $\sqrt{s} = 5.02$ TeV in figure 6. Results for W^- production can be found in figure 11 in the appendix. To highlight the effect of short-distance corrections, we use the `MSHT20nnlo_as118` PDF set for all orders of our predictions in this and in section 3.3.

We neglect negative matching corrections of up to about 3% below 3.16 GeV from α_s^3 contributions. This can amount to an effect of up to about 1.5% in the first bin in the experimental distribution which ranges up to 7 GeV. We show the effect of neglected matching corrections with an additional error bar. Since it is expected that the effect of the neglected matching corrections is negative we plot an error bar of 1.5% only in the negative direction, the amount by which the predictions could shift downwards. Note that our numerical precision in the first bin is similar, at the level of 1%.

Furthermore, towards very small q_T scale uncertainty estimates become potentially unreliable, since a downward variation requires a cutoff to not reach into the non-perturbative regime. This further motivates a symmetrization of uncertainty bars, in addition to the fact that distinguishing between and up- and downwards scale variation is unphysical.

JHEP11(2023)127

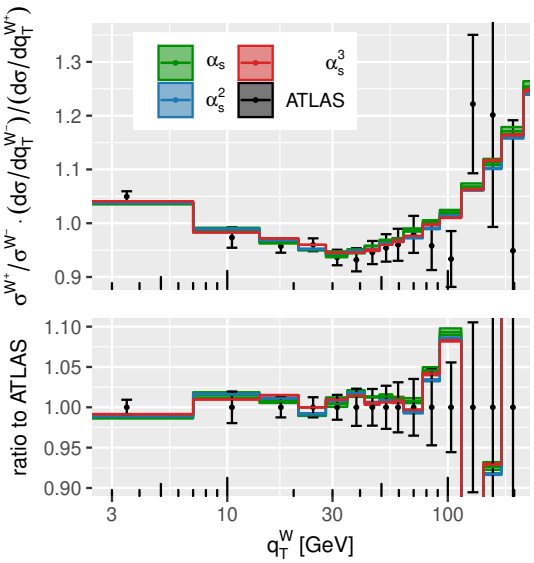

Figure 7. Ratio of W^+/W^- transverse momentum distributions in comparison with the 5.02 TeV ATLAS measurement [17] using the PDF set `MSHT20nnlo_as118` throughout.

Overall the relative corrections are, as expected, very similar to our Drell-Yan results [39] with about 10% corrections in the tail from fixed-order, and smaller corrections at small q_T through higher-order resummation. Uncertainties consistently decrease at higher orders, including the uncertainty associated with transitioning between fixed-order and resummation around 30 GeV to 50 GeV which shrinks considerably at higher orders. The uncertainty bands almost completely overlap between α_s^3 and α_s^2, indicating a stabilization of the perturbative series over the whole range. N^{3}LO effects in the PDF mostly cause a positive shift at small q_T in the first two bins, see section 3.4.

In figure 7 we show the ratio of normalized W^+ to W^- transverse momentum distributions. For this distribution we were able to digitize the plotted ATLAS measurements in ref. [17].[6] We find that the predictions at all orders are compatible within 1% of numerical noise. We also find excellent agreement with the measurement, as already observed in ref. [17].

The agreement of the three perturbative orders within numerical uncertainties indicates that to estimate uncertainties one should compute the ratios in a correlated way, as we have done. This leads to uncertainties smaller than 1%, negligible in comparison with measurement uncertainties and their difference to the predictions.

3.3 Transverse mass and charged lepton transverse momentum distributions

We present the transverse mass distribution for W^+ in figure 8 (left) and for W^- in figure 12 in the appendix. While this distribution could comfortably be computed at fixed order, we only show predictions including the effect of q_T resummation here.

[6]Note that the data for the raw transverse momentum distributions is not available yet, and that we cannot digitize the plot on a logarithmic scale without introducing large errors.

JHEP11(2023)127

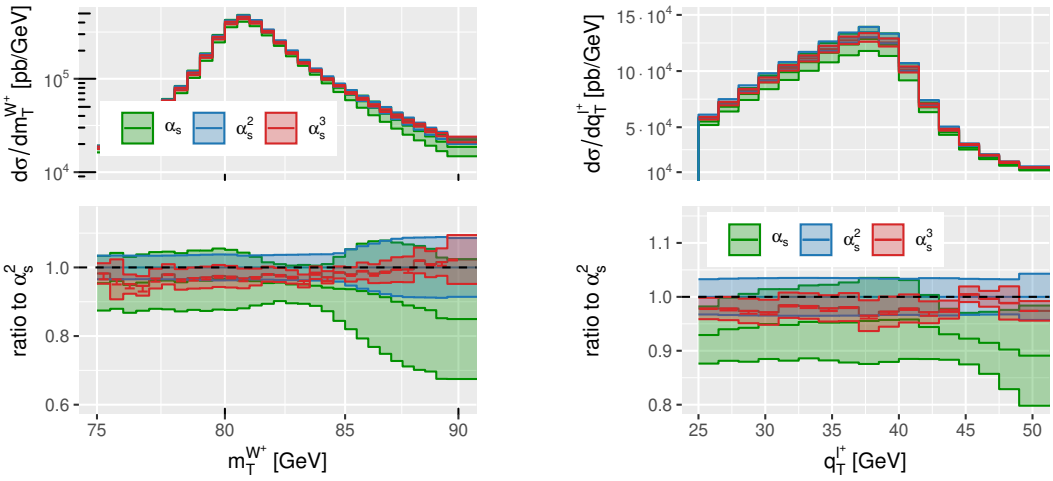

Figure 8. W^+ transverse mass (left) and lepton transverse momentum (right) distributions using the PDF set `MSHT20nnlo_as118` throughout.

.

Perturbative corrections at α_s^3 are flat in the peak region and therefore, as expected from the total fiducial results presented earlier, negative and about 2%. Note that this statement is based on using NNLO PDFs throughout. As we will show in section 3.4, moving towards the aN^{3}LO set, one observes a considerable shift of about 5% below the peak.

In figure 8 (right) we show the W^+ lepton transverse momentum distribution at different orders in α_s (cf. figure 12 in the appendix for W^-). This distribution is particularly important for the W-boson mass determination, since it is sensitive to m_W and does not depend on missing-energy estimations. While typically used in template fits, a new asymmetry observable based on this distribution has recently been proposed in ref. [102].

Within numerical bin-to-bin fluctuations the α_s^3 corrections are flat with smaller uncertainties. This statement also holds while using the aN^{3}LO PDFs and other sets, at least below the peak region.

3.4 Impact of PDFs

As already indicated by the fiducial cross-sections in section 3.1, PDFs are among the biggest limitation in precise predictions. Most insight will be gained by studying differential distributions.

In figure 9 we show the impact of four modern PDF sets for the W^+ transverse momentum, charged lepton transverse momentum, and transverse mass distributions. These relative PDF uncertainties are computed using matched resummed predictions at order α_s^2. The differences to α_s^3 are at the per-mille level and insignificant for this discussion. Even using α_s matrix elements leads to qualitatively the same conclusions [61]. Further, the results for W^- production are virtually the same, but are included for completeness in the appendix in figure 13.

Effects from different PDF sets can be significant, depending on the distribution and region up to 10%. The `MSHT` and `CTEQ` NNLO PDF sets are broadly similar, which are the sets considered in the ATLAS study in ref. [17], in addition to `NNPDF3.1`.

JHEP11(2023)127

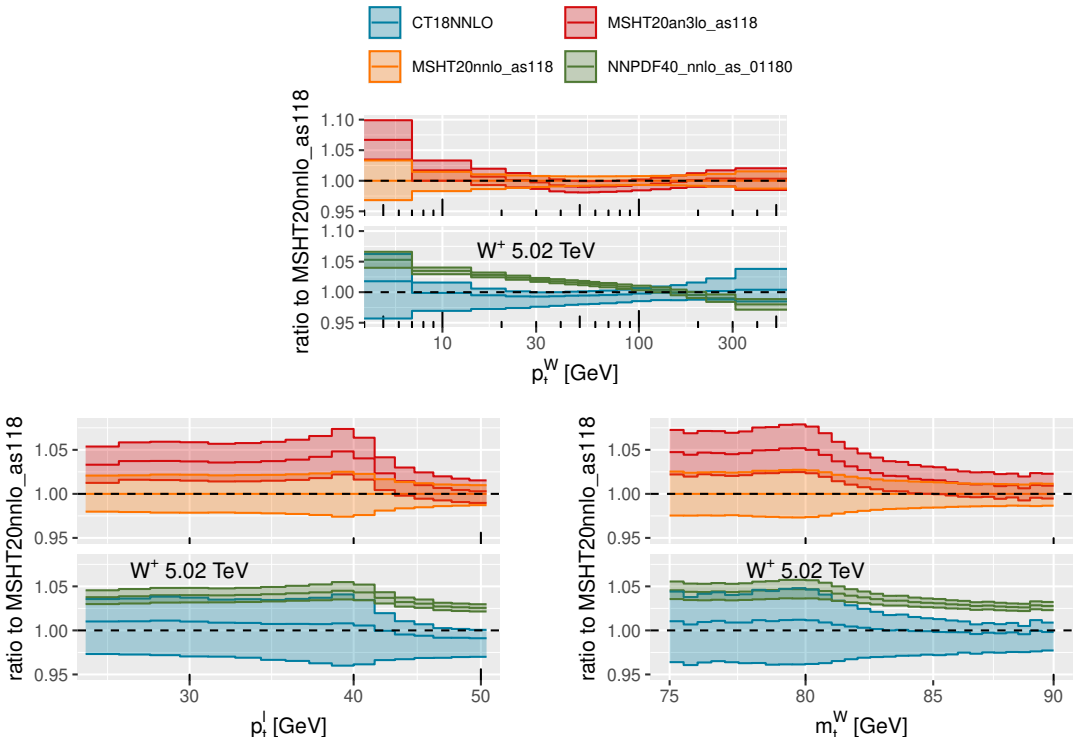

Figure 9. Relative PDF uncertainties of different observables for W^+. Note that `MSHT20an3lo` includes uncertainties from missing higher orders, which are not included in the other sets.

The most interesting comparison is between `MSHT` NNLO and `MSHT` aN^{3}LO as a higher-order effect, and then considering `NNPDF4.0` NNLO. We find significant shape changes for several distributions when utilizing these PDF sets. The effects of using `MSHT` aN^{3}LO are even more important differentially than inclusively since they are non-uniform over the kinematic range. The higher order PDF induces a significant cross-section increase below the peaks for the transverse mass and lepton q_T distributions, while dropping off beyond.

In the W-boson transverse-momentum distribution the most significant change is a positive shift of about 7% in the first bin containing the Sudakov peak, where the bulk of the cross-section resides. This shift is precisely responsible for the better agreement of the total fiducial α_s^2 and α_s^3 cross-sections when the PDF order matches the perturbative short-distance order, see figure 4. This positive shift compensates the negative effect of about -7% at small q_T of the α_s^3 result compared to α_s^2, see figure 6. However this is not a property of the full phase-space since the cross-section increase at large q_T is primarily a result of additional parton radiation.

While the shift of 7% at small q_T is significant, PDF uncertainties even range up to 10%. Clearly such a range can be constrained within QCD uncertainties in future fits, and even precise Drell-Yan measurements and predictions [39] will constrain this significantly.

Predictions using `NNPDF4.0` NNLO for m_t^W and q_T^l are much flatter with respect to `MSHT20` NNLO, except for q_T^W, which predicts a similar enhancement of about 5% in the first bin, but drops off slower than `MSHT20` aN^{3}LO.

JHEP11(2023)127

4 Conclusions & outlook

In recent years the experimental precision of Z and W-boson production has reached new levels at the LHC. In particular this has been achieved through better measurements of the luminosity uncertainty which is now down to 1%. Precise measurements of W-boson kinematics enter many Standard Model inputs like the weak mixing angle, parton distribution functions, and W-boson mass. At the same time, theoretical calculations have become more advanced, reaching new levels of precision in fixed-order and resummed predictions, and allowing for more refined PDF determinations. However these calculations have presented new challenges for performing precision measurements. N^{3}LO QCD corrections are surprisingly large, at the level of minus 2-3% [30] (disregarding the effect of N^{3}LO PDFs), and more statistically precise PDF fits begin to reveal systematic discrepancies that are challenging to reconcile.

Conclusions. In this paper we have presented a calculation of W-boson production at the level of α_s^3 at fixed-order and including the effect of q_T resummation. We find that the size of the total cross-section corrections depends crucially on whether higher-order corrections are included consistently in the short-distance calculation and the PDFs. We considered `MSHT20` PDFs, which, taken at NNLO, lead to results with about -3% corrections at α_s^3. On the other hand using the aN^{3}LO version [63] to consistently match the matrix-element we find that corrections are less than half a percent, which is about our numerical precision. When comparing with data, it seems important to consistently match orders. Other PDF sets like NNPDF4.0 overshoot the experimental measurement at NNLO, but then match it at N^{3}LO due to the large corrections. Whether N^{3}LO effects in other PDF fits lead to a similar increase as for `MSHT20`, and how the systematic differences between them are resolved, will have to be studied in detail in the future.

Our fiducial cross-sections with q_T resummation are overall smaller than at fixed order, but we find larger missing-higher-order uncertainties of about 2.5%. Here in particular the higher-order DGLAP evolution is important to achieve full N^{4}LL accuracy and it is therefore important to match the PDF order.

We calculated differential distributions for the $W^\pm$ transverse momentum, charged lepton transverse momentum and transverse mass distributions. While data for such distributions has not been made public yet, we have digitized the W^+/W^- transverse momentum ratio and found agreement, confirming earlier results at lower orders.

We have illustrated the impact of different PDF sets and their uncertainties for these three kinematic distributions. We find large shape differences between `MSHT20` NNLO and aN^{3}LO, but also between `NNPDF40_nnlo` and the other sets considered. The differences and shape changes reach 5–10%. It is therefore clear that the precise measurements will further strongly constrain PDFs.

In the future it will be interesting to include the effect of non-perturbative corrections in the context of transverse-momentum-dependent PDFs [103–105]. In the typical formalisms the disentangling of perturbative and non-perturbative effects in a model-independent way is difficult [106], but which is simpler here since no direct Landau pole regularization is

JHEP11(2023)127

needed [107]. A further phenomenological avenue will be to study the effect of higher-order resummation on angular coefficients which are used in experimental studies to dress parton-shower results with higher-order corrections.

Our calculation including the matching to W+jet production at NNLO will be publicly available in the upcoming CuTe-MCFM release and allows for theory-data comparison at the state-of-the-art level.

Calculational outlook. While our calculation at N^{3}LO is computationally expensive compared to NLO or NNLO results, which can be computed in a short time on modern multi-core desktops, it is relatively low compared to other state-of-the-art calculations [94]. The precision reached in this paper is about 0.5% for total fiducial cross-sections, and is limited by the double-real W+jet NNLO calculation at small q_T. We have used about 1500 NERSC Perlmutter node hours for this, which translates into about 100,000 core hours.

Unfortunately we are roughly limited to a precision of 0.5% for the chosen set of fiducial cuts which have large matching corrections in the case of resummation, and require small q_T^{cut} values to reach q_T-subtraction asymptotics at fixed order.[7] In our nested slicing approach such small q_T^{cut} values come at the price of correspondingly smaller τ_{cut} in the W+jet NNLO slicing calculation. For example, we estimate that decreasing the cutoff to less than 1 GeV will require an order of magnitude smaller τ_{cut}. Since Monte-Carlo integration uncertainties decrease asymptotically only like $1/\sqrt{N}$, where N is the number of calls (or runtime), one quickly reaches the limit of reasonable runtimes. Future improvements based on local subtractions for the W+jet NNLO calculation, and ultimately for the N^{3}LO cross-section will naturally improve this.

In practice the numerical uncertainty of 0.5% does not pose a problem. In the W-boson q_T distribution it only affects the first bin, typically at the level of 1% but dependent on the exact extent of the bin. In our other resummed distributions it is smeared out and still small compared to our estimation of missing-higher-order uncertainties.

Acknowledgments. We would like to thank NERSC for use of the Perlmutter supercomputer that enabled this calculation. This manuscript has been authored by Fermi Research Alliance, LLC under Contract No. DE-AC02-07CH11359 with the U.S. Department of Energy, Office of Science, Office of High Energy Physics. Tobias Neumann is supported by the United States Department of Energy under Grant Contract DE-SC0012704. This research used resources of the National Energy Research Scientific Computing Center (NERSC), a U.S. Department of Energy Office of Science User Facility located at Lawrence Berkeley National Laboratory, operated under Contract No. DE-AC02-05CH11231 using NERSC award HEP-ERCAP0023824 "Higher-order calculations for precision collider phenomenology".

A Results for W^- production

A comparison of the fiducial cross-section measurement at $\sqrt{s} = 5.02\,\text{TeV}$ with our theoretical predictions for W^- production is shown in figure 10. The relative perturbative corrections to

[7] This 0.5% uncertainty of the total cross-section translates to about a 10% uncertainty of the α_s^3 coefficient itself.

JHEP11(2023)127

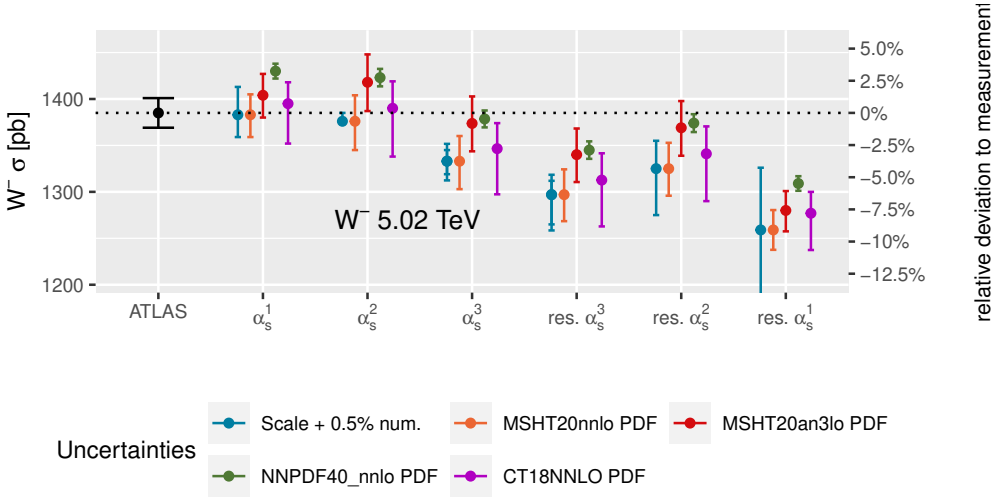

Figure 10. W^- cross-sections in comparison with the ATLAS 5.02 TeV measurement [17]. Error bars show uncertainties from scale variation and from different PDF sets with their respective uncertainties. The α_s^3 results have an additional numerical and cutoff uncertainty of 0.5% that we added linearly to the scale uncertainties.

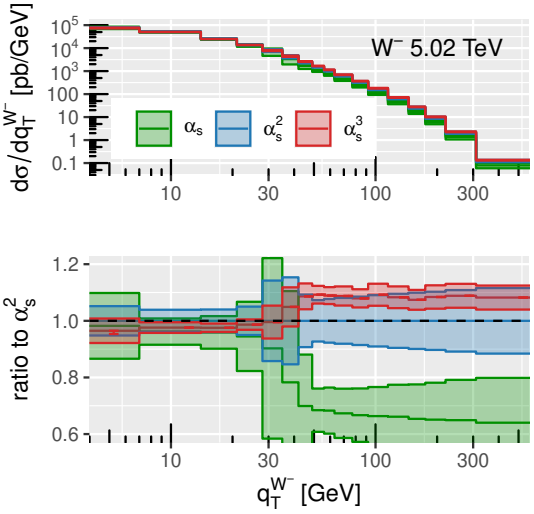

Figure 11. W^- transverse momentum distribution at 5.02 TeV.

the W^--boson transverse momentum (figure 11), the W^--boson transverse mass (figure 12 left), and the charged lepton transverse momentum (figure 12 right) distributions are very similar to the corresponding W^+ results in the main text, see figures 6 and 8. The impact of different PDF fits with uncertainties for W^- distributions is shown in figure 13. We find that the relative positions of the individual predictions shift only slightly compared to W^+ production.

JHEP11(2023)127

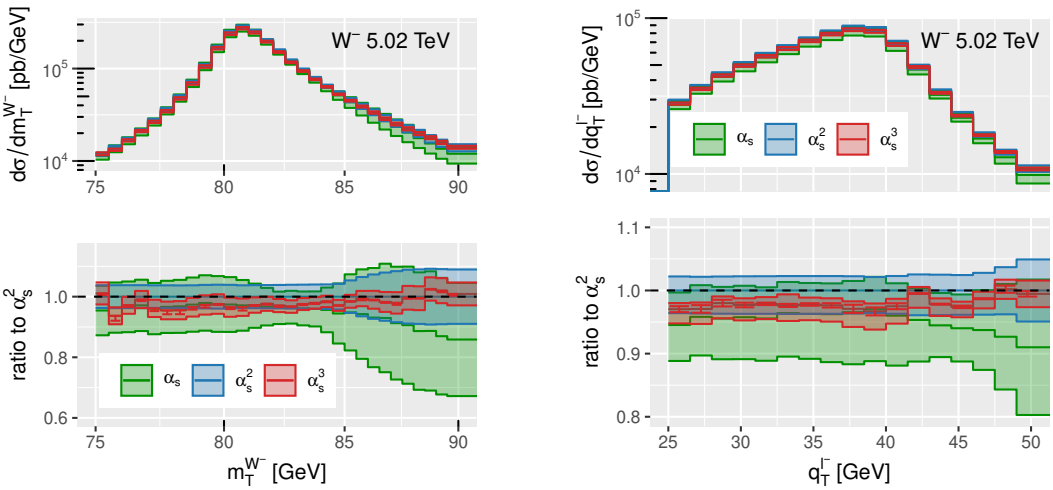

Figure 12. W^- transverse mass (left) and electron transverse momentum (right) distributions at 5.02 TeV.

.

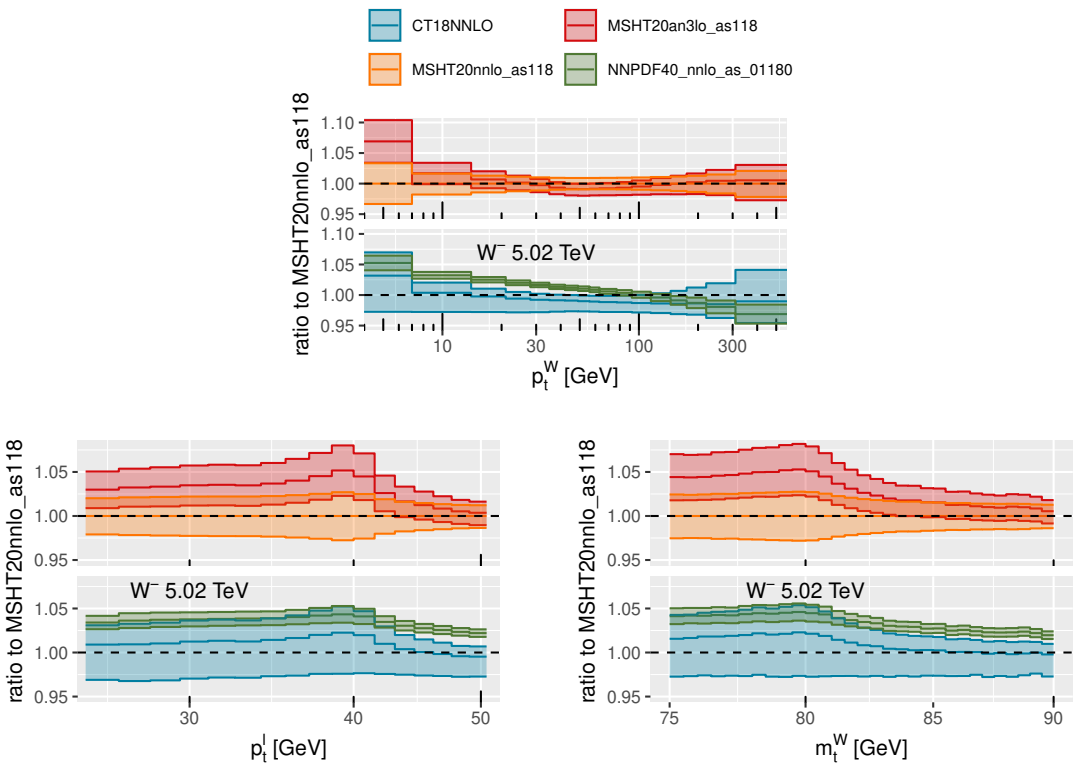

Figure 13. Relative PDF uncertainties of different observables for W^-. Note that `MSHT20an3lo` includes uncertainties from missing higher orders, which are not included in the other sets.

JHEP11(2023)127

References

[1] ATLAS collaboration, *Measurement of $W^{\pm}$-boson and Z-boson production cross-sections in pp collisions at $\sqrt{s} = 2.76$ TeV with the ATLAS detector*, *Eur. Phys. J. C* **79** (2019) 901 [arXiv:1907.03567] [INSPIRE].

[2] ATLAS collaboration, *Measurements of W and Z boson production in pp collisions at $\sqrt{s} = 5.02$ TeV with the ATLAS detector*, *Eur. Phys. J. C* **79** (2019) 128 [*Erratum ibid.* **79** (2019) 374] [arXiv:1810.08424] [INSPIRE].

[3] ATLAS collaboration, *Measurement of differential cross sections and W^+/W^- cross-section ratios for W boson production in association with jets at $\sqrt{s} = 8$ TeV with the ATLAS detector*, *JHEP* **05** (2018) 077 [*Erratum ibid.* **10** (2020) 048] [arXiv:1711.03296] [INSPIRE].

[4] ATLAS collaboration, *Precision measurement and interpretation of inclusive W^+, W^- and Z/γ^* production cross sections with the ATLAS detector*, *Eur. Phys. J. C* **77** (2017) 367 [arXiv:1612.03016] [INSPIRE].

[5] CMS collaboration, *Measurements of differential production cross sections for a Z boson in association with jets in pp collisions at $\sqrt{s} = 8$ TeV*, *JHEP* **04** (2017) 022 [arXiv:1611.03844] [INSPIRE].

[6] CMS collaboration, *Measurement of inclusive W and Z boson production cross sections in pp collisions at $\sqrt{s} = 8$ TeV*, *Phys. Rev. Lett.* **112** (2014) 191802 [arXiv:1402.0923] [INSPIRE].

[7] CMS collaboration, *Measurement of the Inclusive W and Z Production Cross Sections in pp Collisions at $\sqrt{s} = 7$ TeV*, *JHEP* **10** (2011) 132 [arXiv:1107.4789] [INSPIRE].

[8] CMS collaboration, *Measurements of Inclusive W and Z Cross Sections in pp Collisions at $\sqrt{s} = 7$ TeV*, *JHEP* **01** (2011) 080 [arXiv:1012.2466] [INSPIRE].

[9] CMS collaboration, *Measurements of the W boson rapidity, helicity, double-differential cross sections, and charge asymmetry in pp collisions at $\sqrt{s} = 13$ TeV*, *Phys. Rev. D* **102** (2020) 092012 [arXiv:2008.04174] [INSPIRE].

[10] LHCb collaboration, *Measurement of forward $W \to e\nu$ production in pp collisions at $\sqrt{s} = 8$ TeV*, *JHEP* **10** (2016) 030 [arXiv:1608.01484] [INSPIRE].

[11] LHCb collaboration, *Measurement of forward W and Z boson production in association with jets in proton-proton collisions at $\sqrt{s} = 8$ TeV*, *JHEP* **05** (2016) 131 [arXiv:1605.00951] [INSPIRE].

[12] LHCb collaboration, *Measurement of forward W and Z boson production in pp collisions at $\sqrt{s} = 8$ TeV*, *JHEP* **01** (2016) 155 [arXiv:1511.08039] [INSPIRE].

[13] LHCb collaboration, *Measurement of the forward W boson cross-section in pp collisions at $\sqrt{s} = 7$ TeV*, *JHEP* **12** (2014) 079 [arXiv:1408.4354] [INSPIRE].

[14] LHCb collaboration, *Inclusive W and Z production in the forward region at $\sqrt{s} = 7$ TeV*, *JHEP* **06** (2012) 058 [arXiv:1204.1620] [INSPIRE].

JHEP11(2023)127

[15] CMS collaboration, *Precision luminosity measurement in proton-proton collisions at $\sqrt{s} = 13$ TeV in 2015 and 2016 at CMS*, *Eur. Phys. J. C* **81** (2021) 800 [arXiv:2104.01927] [INSPIRE].

[16] ATLAS collaboration, *Luminosity determination in pp collisions at $\sqrt{s} = 13$ TeV using the ATLAS detector at the LHC*, arXiv:2212.09379 [INSPIRE].

[17] ATLAS collaboration, *Precise measurements of W and Z transverse momentum spectra with the ATLAS detector at $\sqrt{s} = 5.02$ TeV and 13 TeV*, ATLAS-CONF-2023-028.

[18] ATLAS collaboration, *Improved W boson Mass Measurement using 7 TeV Proton-Proton Collisions with the ATLAS Detector*, ATLAS-CONF-2023-004 (2023) [INSPIRE].

[19] ATLAS collaboration, *Measurement of the W-boson mass in pp collisions at $\sqrt{s} = 7$ TeV with the ATLAS detector*, *Eur. Phys. J. C* **78** (2018) 110 [*Erratum ibid.* **78** (2018) 898] [arXiv:1701.07240] [INSPIRE].

[20] LHCb collaboration, *Measurement of the W boson mass*, *JHEP* **01** (2022) 036 [arXiv:2109.01113] [INSPIRE].

[21] CDF collaboration, *High-precision measurement of the W boson mass with the CDF II detector*, *Science* **376** (2022) 170 [INSPIRE].

[22] D0 collaboration, *Measurement of the W Boson Mass with the D0 Detector*, *Phys. Rev. Lett.* **108** (2012) 151804 [arXiv:1203.0293] [INSPIRE].

[23] ALEPH et al. collaborations, *Electroweak Measurements in Electron-Positron Collisions at W-Boson-Pair Energies at LEP*, *Phys. Rept.* **532** (2013) 119 [arXiv:1302.3415] [INSPIRE].

[24] ATLAS collaboration, *Determination of the parton distribution functions of the proton from ATLAS measurements of differential $W^{\pm}$ and Z boson production in association with jets*, *JHEP* **07** (2021) 223 [arXiv:2101.05095] [INSPIRE].

[25] CMS collaboration, *Measurement of the Muon Charge Asymmetry in Inclusive $pp \to W + X$ Production at $\sqrt{s} = 7$ TeV and an Improved Determination of Light Parton Distribution Functions*, *Phys. Rev. D* **90** (2014) 032004 [arXiv:1312.6283] [INSPIRE].

[26] ATLAS collaboration, *Measurement of the cross-section and charge asymmetry of W bosons produced in proton-proton collisions at $\sqrt{s} = 8$ TeV with the ATLAS detector*, *Eur. Phys. J. C* **79** (2019) 760 [arXiv:1904.05631] [INSPIRE].

[27] CMS collaboration, *Measurement of the differential cross section and charge asymmetry for inclusive $pp \to W^{\pm} + X$ production at $\sqrt{s} = 8$ TeV*, *Eur. Phys. J. C* **76** (2016) 469 [arXiv:1603.01803] [INSPIRE].

[28] CMS collaboration, *Measurement of the Electron Charge Asymmetry in Inclusive W Production in pp Collisions at $\sqrt{s} = 7$ TeV*, *Phys. Rev. Lett.* **109** (2012) 111806 [arXiv:1206.2598] [INSPIRE].

[29] CMS collaboration, *Measurement of the lepton charge asymmetry in inclusive W production in pp collisions at $\sqrt{s} = 7$ TeV*, *JHEP* **04** (2011) 050 [arXiv:1103.3470] [INSPIRE].

[30] C. Duhr, F. Dulat and B. Mistlberger, *Charged current Drell-Yan production at N^3LO*, *JHEP* **11** (2020) 143 [arXiv:2007.13313] [INSPIRE].

[31] C. Duhr and B. Mistlberger, *Lepton-pair production at hadron colliders at N^3LO in QCD*, *JHEP* **03** (2022) 116 [arXiv:2111.10379] [INSPIRE].

JHEP11(2023)127

[32] A. Gehrmann-De Ridder et al., *Next-to-Next-to-Leading-Order QCD Corrections to the Transverse Momentum Distribution of Weak Gauge Bosons*, *Phys. Rev. Lett.* **120** (2018) 122001 [arXiv:1712.07543] [INSPIRE].

[33] W. Bizon et al., *Momentum-space resummation for transverse observables and the Higgs $p_\perp$ at N^3LL+NNLO*, *JHEP* **02** (2018) 108 [arXiv:1705.09127] [INSPIRE].

[34] P.F. Monni, E. Re and P. Torrielli, *Higgs Transverse-Momentum Resummation in Direct Space*, *Phys. Rev. Lett.* **116** (2016) 242001 [arXiv:1604.02191] [INSPIRE].

[35] W. Bizon et al., *The transverse momentum spectrum of weak gauge bosons at N^3LL + NNLO*, *Eur. Phys. J. C* **79** (2019) 868 [arXiv:1905.05171] [INSPIRE].

[36] S. Camarda, L. Cieri and G. Ferrera, *Drell-Yan lepton-pair production: q_T resummation at N^3LL accuracy and fiducial cross sections at N^3LO*, *Phys. Rev. D* **104** (2021) L111503 [arXiv:2103.04974] [INSPIRE].

[37] E. Re, L. Rottoli and P. Torrielli, *Fiducial Higgs and Drell-Yan distributions at N^3LL' + NNLO with RadISH*, arXiv:2104.07509 [DOI:10.1007/JHEP09(2021)108] [INSPIRE].

[38] X. Chen et al., *Third-Order Fiducial Predictions for Drell-Yan Production at the LHC*, *Phys. Rev. Lett.* **128** (2022) 252001 [arXiv:2203.01565] [INSPIRE].

[39] T. Neumann and J. Campbell, *Fiducial Drell-Yan production at the LHC improved by transverse-momentum resummation at $N^4LLp + N^3LO$*, *Phys. Rev. D* **107** (2023) L011506 [arXiv:2207.07056] [INSPIRE].

[40] W.-L. Ju and M. Schönherr, *The q_T and $\Delta\phi$ spectra in W and Z production at the LHC at N^3LL'+N^2LO*, *JHEP* **10** (2021) 088 [arXiv:2106.11260] [INSPIRE].

[41] S. Camarda, L. Cieri and G. Ferrera, *Drell-Yan lepton-pair production: q_T resummation at approximate $N^4LL + N^4LO$ accuracy*, *Phys. Lett. B* **845** (2023) 138125 [arXiv:2303.12781] [INSPIRE].

[42] M. Bonvini and G. Marinelli, *On the approaches to threshold resummation of rapidity distributions for the Drell-Yan process*, *Eur. Phys. J. C* **83** (2023) 931 [arXiv:2306.03568] [INSPIRE].

[43] G. Das, *$Z, W^\pm$ rapidity distributions at NNLL and beyond*, arXiv:2303.16578 [INSPIRE].

[44] P. Banerjee, G. Das, P.K. Dhani and V. Ravindran, *Threshold resummation of the rapidity distribution for Drell-Yan production at NNLO + NNLL*, *Phys. Rev. D* **98** (2018) 054018 [arXiv:1805.01186] [INSPIRE].

[45] G. Lustermans, J.K.L. Michel and F.J. Tackmann, *Generalized Threshold Factorization with Full Collinear Dynamics*, arXiv:1908.00985 [INSPIRE].

[46] D. Gutierrez-Reyes, S. Leal-Gomez and I. Scimemi, *W-boson production in TMD factorization*, *Eur. Phys. J. C* **81** (2021) 418 [arXiv:2011.05351] [INSPIRE].

[47] X. Chen et al., *Transverse mass distribution and charge asymmetry in W boson production to third order in QCD*, *Phys. Lett. B* **840** (2023) 137876 [arXiv:2205.11426] [INSPIRE].

[48] L. Buonocore et al., *Mixed QCD-EW corrections to $pp \to \ell\nu_\ell + X$ at the LHC*, *Phys. Rev. D* **103** (2021) 114012 [arXiv:2102.12539] [INSPIRE].

[49] A. Behring et al., *Mixed QCD-electroweak corrections to W-boson production in hadron collisions*, *Phys. Rev. D* **103** (2021) 013008 [arXiv:2009.10386] [INSPIRE].

JHEP11(2023)127

[50] S. Dittmaier, T. Schmidt and J. Schwarz, *Mixed NNLO QCD×electroweak corrections of $\mathcal{O}(N_f\alpha_s\alpha)$ to single-W/Z production at the LHC*, *JHEP* **12** (2020) 201 [arXiv:2009.02229] [INSPIRE].

[51] S. Dittmaier, A. Huss and C. Schwinn, *Mixed QCD-electroweak $\mathcal{O}(\alpha_s\alpha)$ corrections to Drell-Yan processes in the resonance region: pole approximation and non-factorizable corrections*, *Nucl. Phys. B* **885** (2014) 318 [arXiv:1403.3216] [INSPIRE].

[52] S. Dittmaier, A. Huss and C. Schwinn, *Dominant mixed QCD-electroweak $O(\alpha_s\alpha)$ corrections to Drell-Yan processes in the resonance region*, *Nucl. Phys. B* **904** (2016) 216 [arXiv:1511.08016] [INSPIRE].

[53] A. Autieri, L. Cieri, G. Ferrera and G.F.R. Sborlini, *Combining QED and QCD transverse-momentum resummation for W and Z boson production at hadron colliders*, *JHEP* **07** (2023) 104 [arXiv:2302.05403] [INSPIRE].

[54] CMS collaboration, *Measurement of the transverse momentum spectra of weak vector bosons produced in proton-proton collisions at $\sqrt{s} = 8$ TeV*, *JHEP* **02** (2017) 096 [arXiv:1606.05864] [INSPIRE].

[55] ATLAS collaboration, *Measurement of the Transverse Momentum Distribution of W Bosons in pp Collisions at $\sqrt{s} = 7$ TeV with the ATLAS Detector*, *Phys. Rev. D* **85** (2012) 012005 [arXiv:1108.6308] [INSPIRE].

[56] C.M. Carloni Calame et al., *Precision Measurement of the W-Boson Mass: Theoretical Contributions and Uncertainties*, *Phys. Rev. D* **96** (2017) 093005 [arXiv:1612.02841] [INSPIRE].

[57] J. Gao, D.Y. Liu and K. Xie, *Understanding PDF uncertainty in W boson mass measurements**, *Chin. Phys. C* **46** (2022) 123110 [arXiv:2205.03942] [INSPIRE].

[58] J. Isaacson, Y. Fu and C.-P. Yuan, *ResBos2 and the CDF W Mass Measurement*, arXiv:2205.02788 [INSPIRE].

[59] A. Behring et al., *Estimating the impact of mixed QCD-electroweak corrections on the W-mass determination at the LHC*, *Phys. Rev. D* **103** (2021) 113002 [arXiv:2103.02671] [INSPIRE].

[60] T. Becher and T. Neumann, *Fiducial q_T resummation of color-singlet processes at N^3LL+NNLO*, *JHEP* **03** (2021) 199 [arXiv:2009.11437] [INSPIRE].

[61] J. Campbell and T. Neumann, *Precision Phenomenology with MCFM*, *JHEP* **12** (2019) 034 [arXiv:1909.09117] [INSPIRE].

[62] T. Neumann, *The diphoton q_T spectrum at $N^3LL' + NNLO$*, *Eur. Phys. J. C* **81** (2021) 905 [arXiv:2107.12478] [INSPIRE].

[63] J. McGowan, T. Cridge, L.A. Harland-Lang and R.S. Thorne, *Approximate N^3LO parton distribution functions with theoretical uncertainties: MSHT20aN^3LO PDFs*, *Eur. Phys. J. C* **83** (2023) 185 [*Erratum ibid.* **83** (2023) 302] [arXiv:2207.04739] [INSPIRE].

[64] T. Becher and M. Neubert, *Drell-Yan Production at Small q_T, Transverse Parton Distributions and the Collinear Anomaly*, *Eur. Phys. J. C* **71** (2011) 1665 [arXiv:1007.4005] [INSPIRE].

[65] T. Becher, M. Neubert and D. Wilhelm, *Electroweak Gauge-Boson Production at Small q_T: Infrared Safety from the Collinear Anomaly*, *JHEP* **02** (2012) 124 [arXiv:1109.6027] [INSPIRE].

JHEP11(2023)127

[66] T. Becher, M. Neubert and D. Wilhelm, *Higgs-Boson Production at Small Transverse Momentum*, *JHEP* **05** (2013) 110 [arXiv:1212.2621] [INSPIRE].

[67] M.-X. Luo, T.-Z. Yang, H.X. Zhu and Y.J. Zhu, *Unpolarized quark and gluon TMD PDFs and FFs at N^3LO*, *JHEP* **06** (2021) 115 [arXiv:2012.03256] [INSPIRE].

[68] M.A. Ebert, B. Mistlberger and G. Vita, *Transverse momentum dependent PDFs at N^3LO*, *JHEP* **09** (2020) 146 [arXiv:2006.05329] [INSPIRE].

[69] M.-X. Luo, T.-Z. Yang, H.X. Zhu and Y.J. Zhu, *Quark Transverse Parton Distribution at the Next-to-Next-to-Next-to-Leading Order*, *Phys. Rev. Lett.* **124** (2020) 092001 [arXiv:1912.05778] [INSPIRE].

[70] C. Duhr, B. Mistlberger and G. Vita, *Four-Loop Rapidity Anomalous Dimension and Event Shapes to Fourth Logarithmic Order*, *Phys. Rev. Lett.* **129** (2022) 162001 [arXiv:2205.02242] [INSPIRE].

[71] I. Moult, H.X. Zhu and Y.J. Zhu, *The four loop QCD rapidity anomalous dimension*, *JHEP* **08** (2022) 280 [arXiv:2205.02249] [INSPIRE].

[72] T. Gehrmann et al., *Calculation of the quark and gluon form factors to three loops in QCD*, *JHEP* **06** (2010) 094 [arXiv:1004.3653] [INSPIRE].

[73] P.A. Baikov et al., *Quark and gluon form factors to three loops*, *Phys. Rev. Lett.* **102** (2009) 212002 [arXiv:0902.3519] [INSPIRE].

[74] R.N. Lee, A.V. Smirnov and V.A. Smirnov, *Analytic Results for Massless Three-Loop Form Factors*, *JHEP* **04** (2010) 020 [arXiv:1001.2887] [INSPIRE].

[75] S. Catani and M. Grazzini, *An NNLO subtraction formalism in hadron collisions and its application to Higgs boson production at the LHC*, *Phys. Rev. Lett.* **98** (2007) 222002 [hep-ph/0703012] [INSPIRE].

[76] R. Boughezal, C. Focke, X. Liu and F. Petriello, *W-boson production in association with a jet at next-to-next-to-leading order in perturbative QCD*, *Phys. Rev. Lett.* **115** (2015) 062002 [arXiv:1504.02131] [INSPIRE].

[77] J. Gaunt, M. Stahlhofen, F.J. Tackmann and J.R. Walsh, *N-jettiness Subtractions for NNLO QCD Calculations*, *JHEP* **09** (2015) 058 [arXiv:1505.04794] [INSPIRE].

[78] I.W. Stewart, F.J. Tackmann and W.J. Waalewijn, *N-Jettiness: An Inclusive Event Shape to Veto Jets*, *Phys. Rev. Lett.* **105** (2010) 092002 [arXiv:1004.2489] [INSPIRE].

[79] J.M. Campbell, R.K. Ellis, R. Mondini and C. Williams, *The NNLO QCD soft function for 1-jettiness*, *Eur. Phys. J. C* **78** (2018) 234 [arXiv:1711.09984] [INSPIRE].

[80] R. Boughezal, X. Liu and F. Petriello, *N-jettiness soft function at next-to-next-to-leading order*, *Phys. Rev. D* **91** (2015) 094035 [arXiv:1504.02540] [INSPIRE].

[81] A. Denner, J.-N. Lang and S. Uccirati, *Recola2: REcursive Computation of One-Loop Amplitudes 2*, *Comput. Phys. Commun.* **224** (2018) 346 [arXiv:1711.07388] [INSPIRE].

[82] T. Gehrmann and L. Tancredi, *Two-loop QCD helicity amplitudes for $q\bar{q} \to W^{\pm}\gamma$ and $q\bar{q} \to Z^0\gamma$*, *JHEP* **02** (2012) 004 [arXiv:1112.1531] [INSPIRE].

[83] L.W. Garland et al., *Two loop QCD helicity amplitudes for $e^+e^- \to$ three jets*, *Nucl. Phys. B* **642** (2002) 227 [hep-ph/0206067] [INSPIRE].

[84] T. Gehrmann and E. Remiddi, *Analytic continuation of massless two loop four point functions*, *Nucl. Phys. B* **640** (2002) 379 [hep-ph/0207020] [INSPIRE].

JHEP11(2023)127

[85] T. Becher, C. Lorentzen and M.D. Schwartz, *Resummation for W and Z production at large pT*, *Phys. Rev. Lett.* **108** (2012) 012001 [arXiv:1106.4310] [INSPIRE].

[86] T. Becher, G. Bell, C. Lorentzen and S. Marti, *Transverse-momentum spectra of electroweak bosons near threshold at NNLO*, *JHEP* **02** (2014) 004 [arXiv:1309.3245] [INSPIRE].

[87] J.M. Campbell and R.K. Ellis, *Next-to-Leading Order Corrections to W^+ 2 jet and Z^+ 2 Jet Production at Hadron Colliders*, *Phys. Rev. D* **65** (2002) 113007 [hep-ph/0202176] [INSPIRE].

[88] A. Gehrmann-De Ridder et al., *NNLO QCD Corrections to W+ jet Production in NNLOJET*, *PoS* **LL2018** (2018) 041 [arXiv:1807.09113] [INSPIRE].

[89] M.A. Ebert, J.K.L. Michel, I.W. Stewart and F.J. Tackmann, *Drell-Yan q_T resummation of fiducial power corrections at N^3LL*, *JHEP* **04** (2021) 102 [arXiv:2006.11382] [INSPIRE].

[90] S. Catani, D. de Florian, G. Ferrera and M. Grazzini, *Vector boson production at hadron colliders: transverse-momentum resummation and leptonic decay*, *JHEP* **12** (2015) 047 [arXiv:1507.06937] [INSPIRE].

[91] T. Becher and M. Hager, *Event-Based Transverse Momentum Resummation*, *Eur. Phys. J. C* **79** (2019) 665 [arXiv:1904.08325] [INSPIRE].

[92] L. Buonocore, S. Kallweit, L. Rottoli and M. Wiesemann, *Linear power corrections for two-body kinematics in the qT subtraction formalism*, *Phys. Lett. B* **829** (2022) 137118 [arXiv:2111.13661] [INSPIRE].

[93] J. Baglio, C. Duhr, B. Mistlberger and R. Szafron, *Inclusive production cross sections at N^3LO*, *JHEP* **12** (2022) 066 [arXiv:2209.06138] [INSPIRE].

[94] F. Febres Cordero, A. von Manteuffel and T. Neumann, *Computational Challenges for Multi-loop Collider Phenomenology: A Snowmass 2021 White Paper*, *Comput. Softw. Big Sci.* **6** (2022) 14 [arXiv:2204.04200] [INSPIRE].

[95] R. Boughezal, A. Isgrò and F. Petriello, *Next-to-leading power corrections to $V+1$ jet production in N-jettiness subtraction*, *Phys. Rev. D* **101** (2020) 016005 [arXiv:1907.12213] [INSPIRE].

[96] F. Caola et al., *The Path forward to N^3LO*, in the proceedings of the *Snowmass 2021*, Seattle U.S.A., July 17–26 (2022) [arXiv:2203.06730] [INSPIRE].

[97] S. Alioli et al., *Precision studies of observables in $pp \to W \to l\nu_l$ and $pp \to \gamma, Z \to l^+l^-$ processes at the LHC*, *Eur. Phys. J. C* **77** (2017) 280 [arXiv:1606.02330] [INSPIRE].

[98] G.P. Salam and E. Slade, *Cuts for two-body decays at colliders*, *JHEP* **11** (2021) 220 [arXiv:2106.08329] [INSPIRE].

[99] S. Bailey et al., *Parton distributions from LHC, HERA, Tevatron and fixed target data: MSHT20 PDFs*, *Eur. Phys. J. C* **81** (2021) 341 [arXiv:2012.04684] [INSPIRE].

[100] T.-J. Hou et al., *Progress in the CTEQ-TEA NNLO global QCD analysis*, arXiv:1908.11394 [INSPIRE].

[101] NNPDF collaboration, *The path to proton structure at 1% accuracy*, *Eur. Phys. J. C* **82** (2022) 428 [arXiv:2109.02653] [INSPIRE].

[102] L. Rottoli, P. Torrielli and A. Vicini, *Determination of the W-boson mass at hadron colliders*, *Eur. Phys. J. C* **83** (2023) 948 [arXiv:2301.04059] [INSPIRE].

[103] V. Moos, I. Scimemi, A. Vladimirov and P. Zurita, *Extraction of unpolarized transverse momentum distributions from fit of Drell-Yan data at N^4LL*, arXiv:2305.07473 [INSPIRE].

JHEP11(2023)127

[104] I. Scimemi and A. Vladimirov, *Non-perturbative structure of semi-inclusive deep-inelastic and Drell-Yan scattering at small transverse momentum*, *JHEP* **06** (2020) 137 [arXiv:1912.06532] [INSPIRE].

[105] A. Bacchetta et al., *Transverse-momentum-dependent parton distributions up to N^3LL from Drell-Yan data*, *JHEP* **07** (2020) 117 [arXiv:1912.07550] [INSPIRE].

[106] M.A. Ebert, J.K.L. Michel, I.W. Stewart and Z. Sun, *Disentangling long and short distances in momentum-space TMDs*, *JHEP* **07** (2022) 129 [arXiv:2201.07237] [INSPIRE].

[107] T. Becher and G. Bell, *Enhanced nonperturbative effects through the collinear anomaly*, *Phys. Rev. Lett.* **112** (2014) 182002 [arXiv:1312.5327] [INSPIRE].

JHEP11(2023)127